

Numerical solutions of the nonlinear α -effect dynamo equations

By MICHAEL R. E. PROCTOR

Department of Mathematics, Massachusetts
Institute of Technology, Cambridge

(Received 2 April 1976 and in revised form 21 September 1976)

An extension is made of the α -effect model of the earth's dynamo into the nonlinear regime following the prescription of Malkus & Proctor (1975). In this model, the effects of small-scale dynamics on the α -effect are suppressed, and the global effects of induced velocity fields examined in isolation. The equations are solved numerically using finite-difference methods, and it is shown that viscous and inertial forces are unimportant in the final equilibration, as suggested in the above paper.

1. Introduction

In a recent paper, Malkus & Proctor (1975, hereinafter referred to as I) have proposed that the constraints that limit the growth of the magnetic field of the earth are global in nature and relatively insensitive to the details of the magnetic regeneration process. It is noted there that the primary force balance in the core of the earth is between Coriolis and Lorentz forces and the pressure gradient, with viscous and inertial forces playing a secondary role. If the regenerating mechanism is relatively insensitive to the growth of the field, the change in the global flow pattern produced by the Lorentz forces should lead to final steady values of the magnetic energy which are $O(\Omega\lambda\mu\rho)$, where Ω is the angular velocity of the core, λ the magnetic diffusivity and μ and ρ the magnetic permeability and density, respectively, of the core fluid. The quantitative analysis of I was confined to the special case $\alpha = \text{constant}$ of the ' α -effect' that models magnetic energy input to the large scales (see I for references). Two regimes are considered there: the 'viscous limit', valid at small field amplitudes, in which viscous effects determine the final equilibration, and the 'inviscid limit', valid for larger fields, when Ohmic loss is the principal equilibrating mechanism. We have discovered errors in the analysis for the latter regime. Specifically, it is proved that the equations in the former case have no steady solution, at third order in the expansion parameter, so that figure 3 of I is incorrect. This means that for $\alpha = \text{constant}$ viscous forces are always important in determining the eventual field size if the solution is steady (although an inviscid oscillatory solution cannot be ruled out).

Solutions to the inviscid problem have been exhibited, however, in certain special cases (Greenspan 1974; Proctor 1975), and the non-existence proof noted above (details of which are in Proctor q.v.) holds only if α is independent of the co-ordinate parallel to the rotation. Since no realistic form of α satisfies this constraint, we expect that solutions exist in most cases of physical relevance. The model investigated here is one such, and the results we obtain demonstrate the approach to the inviscid limit

as viscous and inertial forces become small. Further, this is the first numerical study of the α -effect dynamo equations that is neither confined to the linear regime (e.g. Roberts 1972) nor based on a physically plausible, but arbitrary parameterization of the dynamics (Jepps 1975). Here we suppose α to be a given function, thus suppressing the small-scale consequences of the change in the mean fields to accord with the ideas in I on the importance of global constraints. The equations to be investigated are then those that relate the mean magnetic field to the large-scale flows induced by the mean Lorentz forces.

In the notation of I, these take the form

$$\partial \mathbf{B} / \partial t = \nabla \times (\mathbf{U} \times \mathbf{B}) + \nabla \times (\alpha f \mathbf{B}) + \nabla^2 \mathbf{B}, \quad (1.1a)$$

$$E_M (\partial \mathbf{U} / \partial t + \mathbf{U} \cdot \nabla \mathbf{U}) + \nabla p + 2\mathbf{k} \times \mathbf{U} = \nabla \times \mathbf{B} \times \mathbf{B} + E \nabla^2 \mathbf{U}, \quad (1.1b)$$

$$\nabla \cdot \mathbf{B} = \nabla \cdot \mathbf{U} = 0, \quad (1.1c)$$

where αf is the presumed magnetic energy source due to small-scale effects, \mathbf{B} is the magnetic field, \mathbf{U} the induced large-scale velocity field and p the pressure. The two dimensionless parameters E and E_M are given by

$$E = \nu / \Omega L^2, \quad E_M = \lambda / \Omega L^2, \quad (1.2)$$

where L is the core radius. Both these numbers are thought to be extremely small for the core (10^{-6} or less). Because of this, an immediate decision had to be made: whether to retain the small terms in E and E_M or whether to attempt to solve the reduced equations obtained by neglecting these terms. The first path has the advantage that the equations are fully predictive, and so permit the full initial-value problem to be solved, at least within the restrictions imposed by the numerical scheme. Its disadvantage lies in the fact that, because of the small coefficient multiplying $\partial \mathbf{U} / \partial t$, the time stepping must proceed very slowly to accommodate any effects with a small time scale that may arise. On the other hand, the second path has the advantage that there are now no small time scales, so that the computation can proceed much more rapidly, but the equations are no longer predictive, so that an arbitrary initial state is not permitted. Specifically, the reduced version of (1.1b),

$$\nabla p + 2\mathbf{k} \times \mathbf{U} = \nabla \times \mathbf{B} \times \mathbf{B}, \quad (1.3)$$

admits solutions for \mathbf{U} if and only if

$$\int_{C(s)} (\nabla \times \mathbf{B} \times \mathbf{B})_\phi d\phi dz \equiv 0, \quad (1.4)$$

where $C(s)$ is any cylinder of radius s coaxial with the angular velocity vector \mathbf{k} (Taylor 1963). Hence (1.4) must be satisfied by any initial state, and remains true for all time. Although such an initial-value problem can certainly be formulated, there is some doubt as to whether a state in which (1.4) is satisfied can ever be attained from a general initial configuration. Roberts & Stewartson (1975) have suggested that the 'Taylor state' may well be unstable under some circumstances, leading to persistent oscillations on a fast Alfvén-wave time scale.

With these observations in mind, we decided that a first study of these equations should include all the terms. We chose a simple form of $f(\cos \theta)$ that was antisymmetric about the equator $z = 0$, and by varying the parameters E and E_M for this case, we could establish whether an asymptotic state was attained as $E, E_M \rightarrow 0$, and acquire some information about the stability of this state. The magnitude of α was taken as

known and independent of the magnetic energy in the large-scale field. This was done in order to study the large-scale equilibration effect in isolation, since a correct parameterization of the effects of α on the large-scale field is not available, and it seems likely that the relative importance of the two mechanisms depends on the type of small-scale forcing used. [The most recent work is that of Busse (1975), who has shown that a modified, anisotropic α -effect can result from small-scale convection in a rotating fluid, and has found an equilibration based on changes in the effective α . In his model, however, there are no large-scale motions at all,† although it can be proved (Proctor 1975) that they *must* occur in a contained body of fluid.] Thus the work presented here is but one side of the coin: a full synthesis lies in the future. Specifically, we examined three cases: $(E, E_M) = (1.0, 1.0)$, $(0.1, 0.04)$ and $(0.005, 0.0025)$. It was hoped that the last of these cases would be well into the presumed asymptotic range prevailing in the geodynamo. For each case, the equations were solved for various values of α by marching forward in time from some initial state until a steady state was reached. Contour plots of the various magnetic and velocity fields involved were produced at given intervals. The magnetic energy M of the toroidal field, used as a measure of the amplitude of the system, was monitored at every time step, so that the approach to the steady state could be examined.

Section 2, then, contains a formulation of the numerical problem and details of the finite-difference scheme used to solve it. Section 3 contains a description of the results obtained in the three cases, and in § 4 the results are evaluated and work in progress is described. Before proceeding with this programme, we may briefly anticipate the conclusions. These are that an asymptotic state in which Taylor's condition holds does indeed occur, and that it appears to be stable, although perhaps not asymptotically stable in the third case considered. Although the computations are all in the weakly nonlinear range, so that the magnetic field is not much altered by changing α , the evolved velocity fields show great differences depending on the relative importance of Coriolis and viscous forces; there is no evidence, however, of the magnetic boundary layer and large zonal flows proposed by Braginskii (1975, 1976) as an alternative to Taylor's prescription.

2. Formulation and numerical methods

Formulation

We seek axisymmetric solutions to (1.1) within a sphere of radius 1. In order to specify the problem fully, we need boundary conditions at the surface $r = 1$. We suppose that the boundary is stress free; this condition is chosen to minimize the effects of viscosity. The boundary condition on the magnetic field is obtained by supposing that the exterior of the sphere is electrically insulated; that is, $\nabla \times \mathbf{B} \equiv 0$ in this region and $|\mathbf{B}| = O(|\mathbf{r}|^{-3})$ as $|\mathbf{r}| \rightarrow \infty$. \mathbf{B} is continuous across the interface $|\mathbf{r}| = 1$. We must now write (1.1) in a manner that will facilitate computation. As in I, we set

$$\mathbf{B} = b\hat{\mathbf{e}}_\phi + \nabla \times (a\hat{\mathbf{e}}_\phi), \quad (2.1a)$$

$$\mathbf{U} = v\hat{\mathbf{e}}_\phi + \nabla \times (\psi\hat{\mathbf{e}}_\phi), \quad (2.1b)$$

$$\nabla \times \mathbf{U} = \omega\hat{\mathbf{e}}_\phi + \nabla \times (v\hat{\mathbf{e}}_\phi), \quad (2.1c)$$

† This does not violate the consistency of Busse's results, since his model is unbounded at leading order.

where $\hat{\mathbf{e}}_\phi$ is a unit vector in the ϕ direction. (This representation uses the solenoidality of \mathbf{U} and \mathbf{B} .) We may now 'uncurl' the meridional part of (1.1a) and eliminate p by taking the curl of the meridional part of (1.1b). These give

$$\partial a / \partial t = N(\psi, a) + \alpha f b + D^2 a \quad (2.2a)$$

and

$$\frac{\partial \omega}{\partial t} = M(v, v) - M(\omega, \psi) + E_M^{-1} \left[2 \frac{\partial v}{\partial z} + ED^2 \omega - M(b, b) - M(D^2 a, a) \right], \quad (2.2b)$$

where $D^2 \equiv \nabla^2 - 1/r^2 \sin^2 \theta$ and the nonlinear terms take the form

$$\left. \begin{aligned} N(x, y) &= \hat{\mathbf{e}}_\phi \cdot (\nabla \times (x \hat{\mathbf{e}}_\phi) \times \nabla \times (y \hat{\mathbf{e}}_\phi)), \\ M(x, y) &= \hat{\mathbf{e}}_\phi \cdot \nabla \times (x \hat{\mathbf{e}}_\phi \times \nabla \times (y \hat{\mathbf{e}}_\phi)). \end{aligned} \right\} \quad (2.3)$$

The remaining three equations come from the ϕ components of (1.1a, b), i.e.

$$\left. \begin{aligned} \partial b / \partial t &= M(v, a) - M(b, \psi) + \alpha \nabla \times (f \nabla \times (a \hat{\mathbf{e}}_\phi)) \cdot \hat{\mathbf{e}}_\phi + D^2 b, \\ \partial v / \partial t &= N(\psi, v) + E_M^{-1} [2 \partial \psi / \partial z + ED^2 v + N(b, a)], \end{aligned} \right\} \quad (2.4)$$

and the elliptic equation connecting ψ and ω , i.e.

$$\omega = -D^2 \psi. \quad (2.5)$$

For $|\mathbf{r}| \geq 1$, the zero-current condition implies

$$D^2 a = 0, \quad b = 0. \quad (2.6)$$

The boundary conditions can therefore be written as

$$\left. \begin{aligned} a, b, \omega, r, \psi &\rightarrow 0 \quad \text{as } |\mathbf{r}| \rightarrow 0, \\ [a] = [\partial a / \partial r] &= 0 \quad \text{across } r = 1, \\ b = \psi = 0, \quad \frac{\partial}{\partial r} \left(\frac{v}{r} \right) &= 0, \quad \omega = 2 \frac{\partial \psi}{\partial r} \quad \text{on } r = 1. \end{aligned} \right\} \quad (2.7)$$

The condition on ψ implies no normal velocity on $r = 1$, and the conditions on v and ω represent the boundary condition of zero tangential stress.

The problem (1.1) has now been reduced to four one-component parabolic equations and one elliptic equation. It should be noted that there are only two types of nonlinear term and only one type of diffusive term when the equations are expressed in this way. These convenient results are used in the program.

Numerical methods

It may be directly observed that it is necessary to solve (2.2), (2.4) and (2.5) only in the hemisphere $z \geq 0$. This is because, for f an odd function of z , the solutions can be divided into dipole (a, v even; b, ψ, ω odd) and quadrupole modes. Hence the region $z < 0$ can be replaced by suitable symmetry conditions at the 'equator' $z = 0$ ($\theta = \frac{1}{2}\pi$). We consider only dipole modes in the present study.

All the variables are held at the nodes of a polar co-ordinate mesh with spacing $(\Delta r, \Delta \theta)$, where $\Delta r = 1/N$ and $\Delta \theta = \pi/2N$. The time step is denoted by Δt . The equations are solved by replacing them with finite-difference analogues that are centred in space and time and have second-order accuracy. The linear terms were

constructed according to the principles of Moore, Peckover & Weiss (1973, hereinafter referred to as MPW), using a centred leapfrog scheme for the time derivative and a formulation for the diffusive term analogous to the DuFort–Frankel scheme for Cartesian meshes. This scheme is explicit, unconditionally stable, and accurate if $\Delta t \leq \frac{1}{2}(1 + 4/\pi^2)^{-1}\Delta r^2$. We were unable to find conservative formulations for the nonlinear terms that are accurate near $r = 0$. The difficulty resides in the averaging procedure of MPW when applied to a non-Cartesian mesh. Details of this problem are given in Proctor (1975). We resolved the difficulty by choosing schemes that were accurate but not conservative for the nonlinear terms. All the schemes used are given in appendix A. In contrast to MPW, and to Weir (1976), who use a staggered mesh, we hold all variables at all points of the mesh. This avoids any difficulties of implementation on the axis, and makes the use of the non-local boundary condition on a much simpler.

The elliptic equation for ψ is solved by successive over-relaxation at each time step. The boundary condition on a can be cast into the form of a time-independent matrix that connects the values of a on $r = 1$ with those in the two adjacent shells. Full details of the method, originally due to P. H. Roberts, may be found in Proctor (1975) and Jepps (1975).

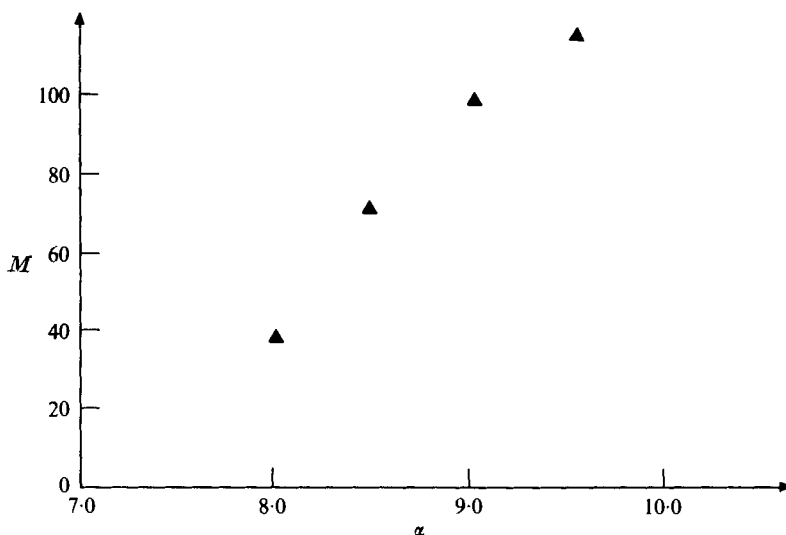
The boundary condition on v has to be chosen to conserve angular momentum as well as possible (the difference scheme is not conservative, so that, although this quantity is an invariant of the full equations, it is not conserved by their discrete form). To this end, we adopted a single-parameter family of relations connecting v at $r = 1$ with interior values, all of which were correct to second order. The free parameter was then varied for each run to minimize the drift of angular momentum. It should be noted, though, that as some drift did occur in spite of these precautions, the angular momentum contours produced by the program are not directly comparable. The steady state reached by the magnetic and poloidal velocity fields was unaffected by this problem.

In actual implementation N was set to 20. All quantities were held at two time levels except ψ (one level) and a (three levels). The three levels for a were necessary to ensure the correct representation of the last term in (2.2*b*) on the boundary; a discussion appears in appendix B. For each run Δt was selected as the largest value compatible with the Dufort–Frankel criterion (see above) and the Courant–Friedrichs–Levy stability criterion

$$U\Delta t/\Delta x \leq 1, \quad (2.8)$$

where U is a typical advection velocity. Both these conditions become rather restrictive when E and $E_M^{\frac{1}{2}}$ are small; $\Delta t = \frac{1}{1200} E_M^{\frac{1}{2}}$ seemed to be sufficient for accuracy and stability. The program required 200k of store on the IBM 370/165 at Cambridge University; a typical time step took about 0.5–0.75 s of computer time.

The system was usually started from a previously evolved steady state with different parameters and was allowed to march forward in time until evolution had ceased. Contour plots were made of all the fields, using a program kindly supplied by Dr D. R. Moore. At the end of each run, a graph was drawn of M against time. This quantity was used in I as a measure of magnetic field strength. The results of these investigations are presented in the following section.

FIGURE 1. M as a function of α for case (i).

3. Results

Preamble

The results described in this section were all obtained for $f = \cos \theta$. This form of f has the required antisymmetry about $\theta = \frac{1}{2}\pi$ and is one of the models whose linear eigensolution was obtained by Roberts (1972) in his comprehensive study of kinematic α -effect dynamos.

An advantage of the model was that the magnetic fields produced were relatively slowly varying in space, so that only a moderate number of mesh points were necessary for an adequate representation. Almost all the other models treated by Roberts have the toroidal field confined to regions near the poles, with much greater average curvature. This model was solved for various values of α for three different pairs of values of E_M and E :

- (i) $E_M = E = 1.0$,
- (ii) $E_M^{\frac{1}{2}} = 0.2$, $E = 0.01$,
- (iii) $E_M^{\frac{1}{2}} = 0.05$, $E = 0.005$.

In case (i), the inertial terms and Coriolis terms in (1.1) are comparable and the viscous forces should dominate both these effects owing to the higher derivatives attached to the viscous term. The second and third cases were chosen so that Coriolis forces appeared dominantly in the scaling. If the solutions were similar in these two cases, support would be lent to the hypothesis that the system was near to an asymptotic 'magnetostrophic' state in which $E, E_M \rightarrow 0$ (as envisaged by the original scaling). This conjecture is, we believe, borne out by the results presented below. There are striking differences between the flow patterns in case (i) on the one hand and cases (ii) and (iii) on the other, which reflect the differences in the processes connecting the fields.

In every case, the marching process was continued until no further development occurred in times comparable with the Ohmic decay time of the system, and we believe

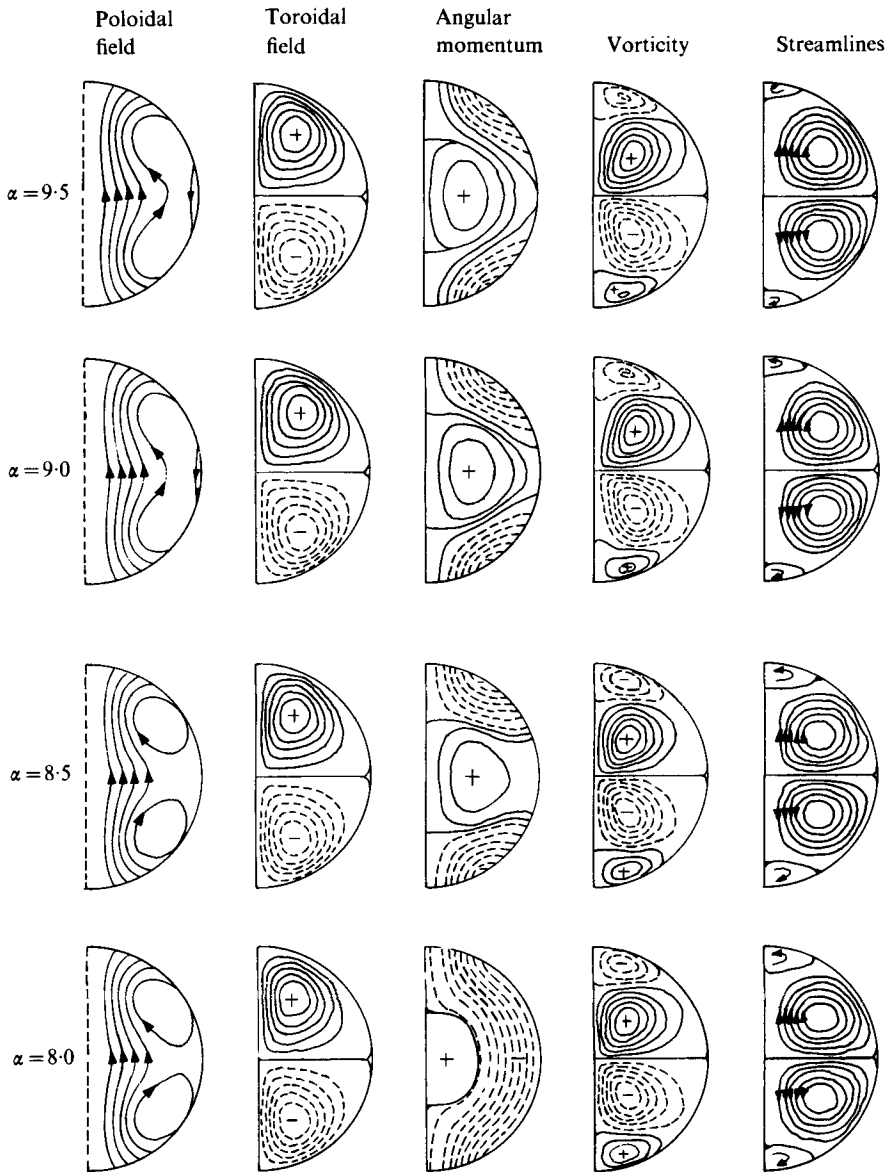


FIGURE 2. Field contours for $E_M^{\frac{1}{2}} = E = 1.0$ (case (i)). From left to right, contours of $ar \sin \theta$, b , $vr \sin \theta$, ω and $\psi r \sin \theta$.

that our values for the equilibrium values of M are accurate to within three significant figures.

In the following three subsections, we discuss the three cases in turn. Finally, in a conclusion, we synthesize our findings and evaluate their significance.

Case (i): $E_M^{\frac{1}{2}} = E = 1.0$

Solutions were obtained for $\alpha = 8.0(0.5)9.5$ according to table 1 below. The first case to be run was $\alpha = 8.5$; it was started from a state of zero velocity and small magnetic

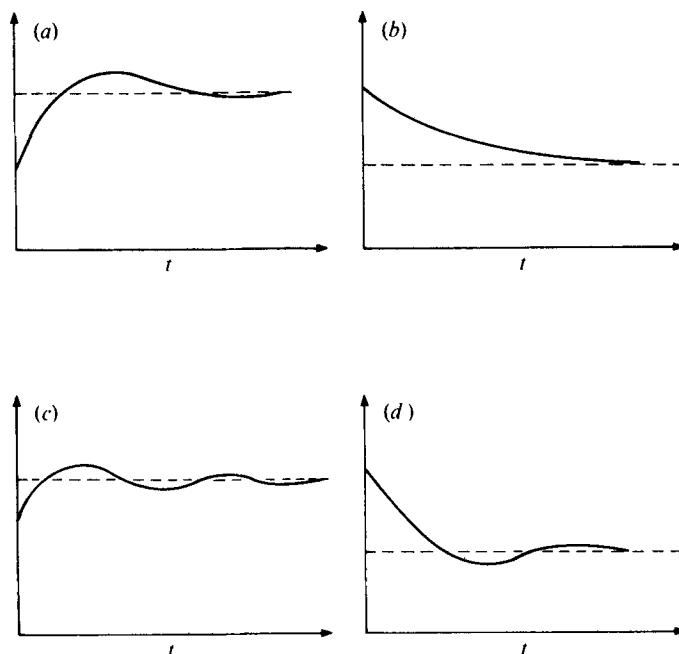


FIGURE 3. Sketches of M as a function of time. (a) Case (i), increased α . (b) Case (i), decreased α . (c) Case (ii), increased α . (d) Case (ii), decreased α .

field approximating the linear eigensolutions. Other cases were started from the state for the next lower value of α except for the case $\alpha = 8.0$, which was started from the state for $\alpha = 9.5$ to investigate a field decaying to its steady state. Figure 1 shows M as a function of α , figure 2 gives contours of the various fields in the steady state and figure 3 is a sketch of typical time development of M . In each case, convergence was achieved after about 1200 time steps, or just over one Ohmic decay time; this high rate is due to the importance of viscous decay in the system (see below). It is clear from figure 3 that the equilibrium amplitudes are smoothly varying functions of α . A good fit to the plotted points is the parabola

$$\alpha = 7.67 + 0.0064M + 7.8 \times 10^{-5}M^2 + \dots, \quad (3.1)$$

so that the intercept on the α axis is pleasingly close to the linear eigenvalue 7.65 found by Roberts. It should be noticed that M is rather large compared with unity even for α as small as 8.0. This is a consequence of the fact that for this case viscous forces act as the principal balance to Lorentz forces ($\nabla^2 \mathbf{U} = O(25|\mathbf{U}|)$ in this geometry). It is easily seen that the larger the value of E , the smaller the $|\mathbf{U}|$ needed for this force balance. Hence there is a weaker back-reaction on the field, which can thus grow to greater amplitude. Indeed, it is easy to show from the equations that in the limit $E \rightarrow \infty$ we must have, for $|\mathbf{B}| = O(1)$,

$$\alpha - \alpha_0 = O(E^{-1}), \quad |\mathbf{U}| = O(E^{-1}), \quad \{E\mathbf{U} \cdot \nabla^2 \mathbf{U}\} = O(E^{-1}), \quad (3.2)$$

where α_0 is the eigenvalue of the linear problem. This rather paradoxical result shows the inconsistency of the model for large E , since in reality α depends on the viscosity, and would presumably be zero for E sufficiently large.

α/M	(i)	(ii)	(iii)
7.9	—	1.27	—
8.0	36.2	1.41	1.42
8.5	70.5	1.88	1.84
9.0	96.4	2.26	2.08
9.5	113.5	2.56	—
10.0	—	2.93	—

TABLE 1. Equilibrium values of M as a function of α in the three cases (i) $E_M^\dagger = E = 1.0$, (ii) $E_M^\dagger = 0.2$, $E = 0.01$ and (iii) $E_M^\dagger = 0.05$, $E = 0.005$.

In the runs for which α was increased, the value of M overshoots its final equilibrium value before approaching it from below; the variation of a with time appears to be 90° out of phase with that of b . When α was *reduced* to 8.0 for the final run, however, all the variables decayed monotonically to their eventual steady state. From the plots, it is clear that the maximum effects of the Lorentz force are at fairly low latitudes, leading to clockwise meridional flow for $z > 0$ and a region of reversed flow near the axis that would seem to play a passive role. There is a region of positive angular momentum near the equator, and a negative jet at mid-latitudes near the boundary (which is, it will be recalled, stress free). This coincides with the place where gradients of both a and b are large. The case $\alpha = 8.0$, run after the other three, shows the effect of angular-momentum drift, but it is clear from the other field contours that the drift does not make any difference to the equilibrium value.

Case (ii): $E_M^\dagger = 0.2$, $E = 0.1$

This case was the most comprehensively studied of the three considered. Runs were made for five values of α between 7.9 and 10.0. We found that this range took us out of the regime where the fields varied in size but not in shape, in contrast to case (i). In making the runs, Δt was set at 0.0004; this was sufficiently short to allow proper resolution of one of the most interesting features of this case: damped oscillations about the steady state. As mentioned in §1, these oscillations were predicted by Braginskii (1970), Roberts & Soward (1972) and Proctor (1975) as likely to occur during the process of setting up a state in which Taylor's condition is satisfied: the theory shows that they are torsional oscillations of concentric cylinders centred on the axis of rotation, with the radial field component B_r acting as the link between the cylinders. The time scale of the oscillations predicted by the theory is E_M^\dagger times the Ohmic decay time.

In all five runs for this case oscillations in M were observed in the approach to the steady state (figure 3 shows a typical development). Their period is approximately $0.8 E_M^\dagger$, lending support to the hypothesis that they are of the Braginskii type. The fact that these oscillations are present at all provides powerful evidence that a magnetostrophic state is being approached, since there seem to be no other mechanisms permitted that allow oscillations on this fast a scale. The first run of this series (for $\alpha = 8.0$) was started from an initial state of no motion, and the oscillations in this case were of an amplitude comparable with the steady-state values of M , remaining significant for four periods before disappearing owing to Ohmic and viscous loss. In the other runs, the oscillations, though of comparable period, were much weaker and

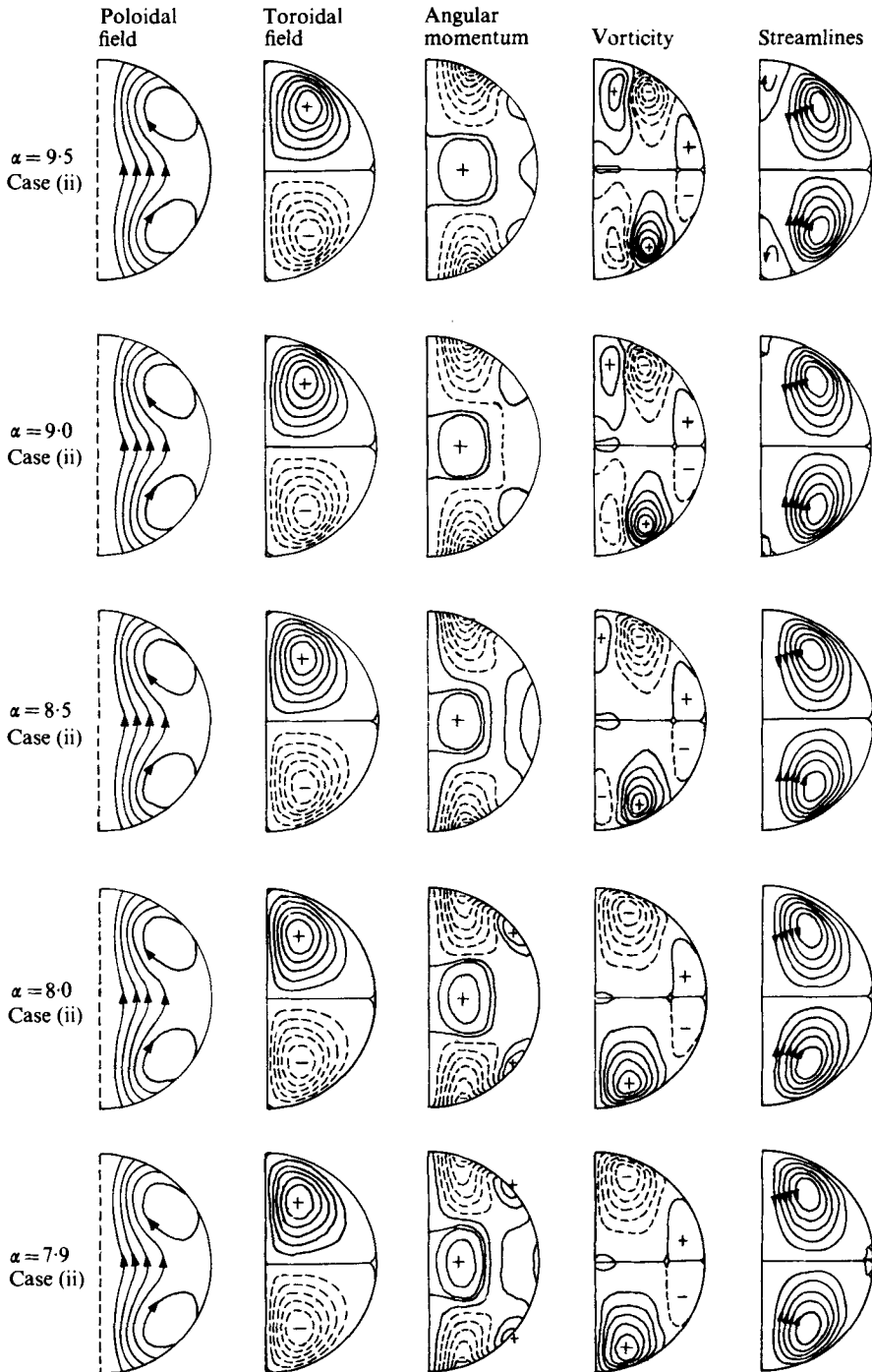


FIGURE 4. For legend see facing page.

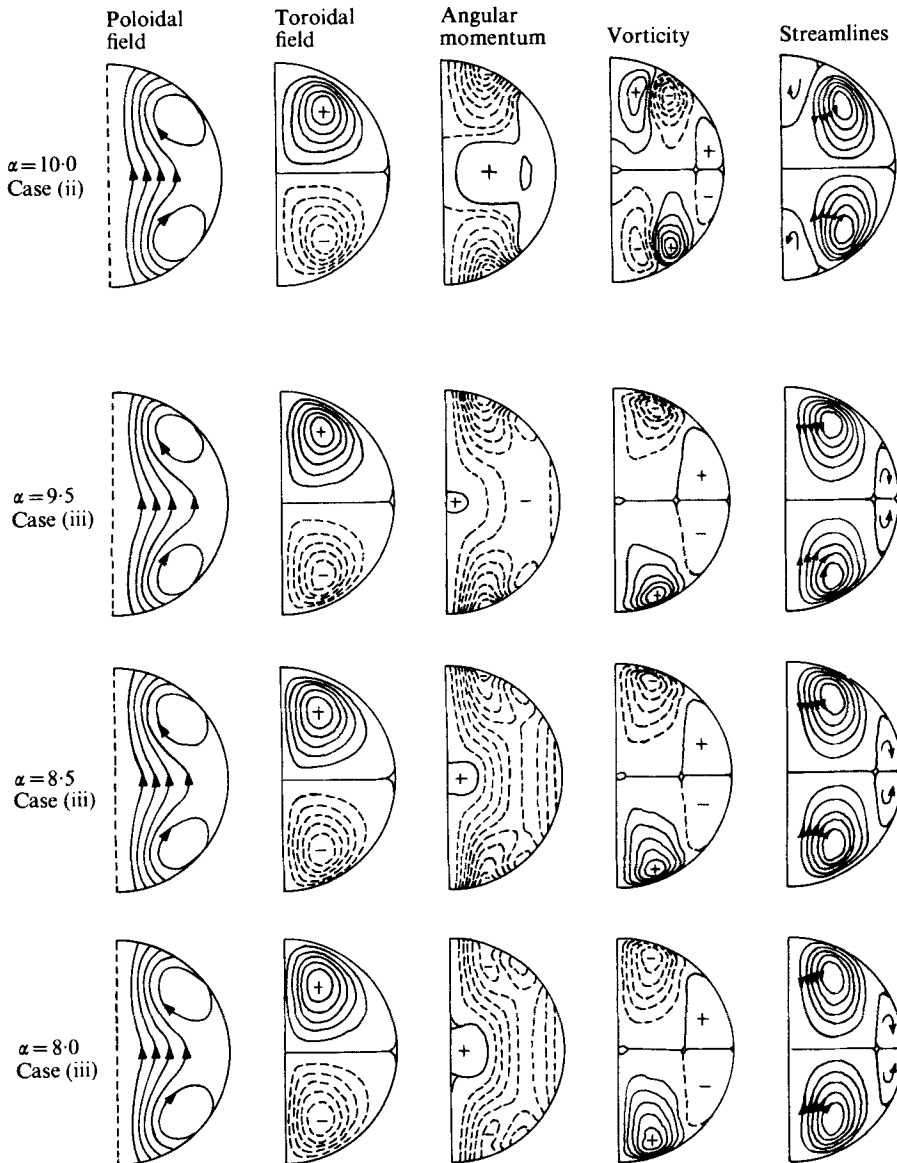


FIGURE 4. Field contours for cases (ii) and (iii).

persisted for only one or two periods; in contrast to case (i), there seemed to be no difference in the character of the oscillations when α was decreased rather than increased.

In table 1 we give the steady-state values of M as a function of α for this case. Contours of the evolved fields are shown in figure 4(a) while figure 5 is a plot of the values in the table.

Our first observation is that the equilibrium values of M are much smaller than for case (i). This shows, as anticipated, that the Coriolis forces are much more potent

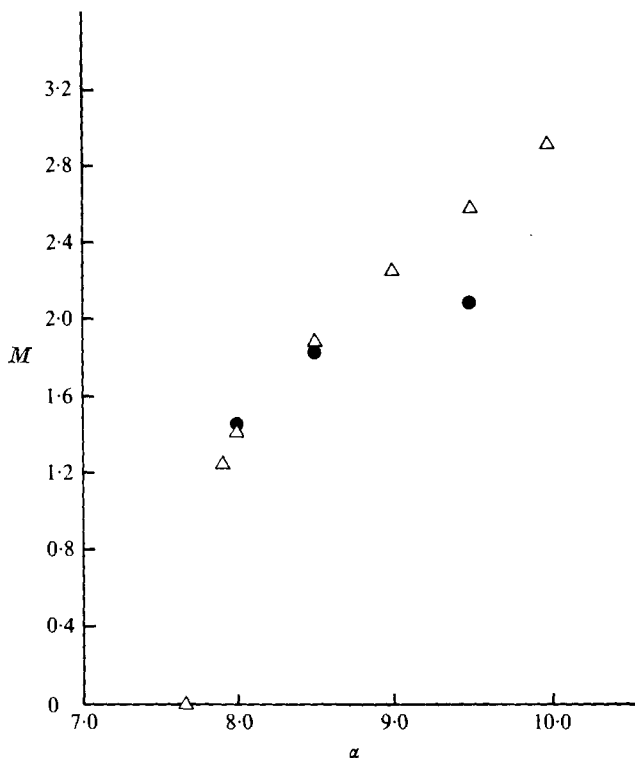


FIGURE 5. M as a function of α . Δ , case (ii) ($E_M^{\frac{1}{2}} = 0.2$, $E = 0.01$); \bullet , case (iii) ($E_M^{\frac{1}{2}} = 0.5$, $E = 0.005$).

than viscous forces at inducing equilibration. We can also see that M rises very rapidly from zero, initially, so that if α can be written as

$$\alpha = 7.65 + kM \quad (3.3)$$

then k is very small. (It is most unlikely that k is exactly zero, since, as shown in I, k comes from the integral of an even function of z involving the linear eigensolution and its adjoint, which is not zero in general.) This seems to be a peculiar feature of the model we chose and it is therefore not well suited to the discovery of subcritical instabilities. For, as noted by Proctor (1975), for every function f giving $k > 0$, the case with $f \rightarrow -f$ has $k < 0$, and hence is subcritically unstable. Fitting a parabola to the first three points the curve gives

$$\alpha = 7.55 - 0.25M + 0.426M^2 \dots, \quad (3.4)$$

so it is possible that k is negative in this case. It would be pointless to make any stronger claim since no steady states have been obtained for $\alpha < 7.65$.

The most noticeable difference between the results for cases (i) and (ii) is that the velocity field in meridional planes has changed sign, at least away from the equator. The driving is now much more clearly concentrated at high latitudes, and the beginnings of boundary-layer structure can be observed in the vorticity, indicating the secondary role that is beginning to be played by the viscosity. Most of the negative angular momentum is concentrated in two jets near the poles; as in case (i), there is a

region of positive angular momentum at the equator. At higher values of α , changes begin to appear in the meridional flow field. This is due to the increased importance of inertial forces in this range, as they are quadratic in $|\mathbf{U}|$. The magnetic fields remain almost the same throughout. There is evidence of the z -independent structure associated with magnetostrophy, in the vertical tendency of contours of the angular momentum. Indeed, we should expect, at very low amplitudes, that this quantity would be almost independent of z since the largest component will be $sv_0(s)$, the free geostrophic flow that results from Taylor's constraint (see I).

$$\text{Case (iii): } E_M^{\frac{1}{2}} = 0.05, E = 0.005$$

This case was, we felt, close to the practical computing limits imposed by the disparity of time scales of the problem. In order to resolve all the phenomena occurring on a fast time scale adequately, we were forced to choose $\Delta t = 0.0002$, and about 1 h of computer time was required to achieve a steady state for each run. For these reasons, we examined only three values of α (8.0, 8.5 and 9.5). If the system is close to the asymptotic state where $E_M^{\frac{1}{2}}, E \rightarrow 0$ we should expect the equilibrium values for this case to be close to those for case (ii). This expectation was borne out by the results, at least for the smaller values of α , and we are therefore confident that an asymptotic magnetostrophic state exists for this form of f . Table 1 shows the final value of M for each α ; field contours are plotted in figure 4(b) and the values in the table are shown in figure 5 alongside those for case (ii).

Clearly, the first two entries in the table are almost identical to the corresponding ones for the previous case. Comparison of the field contours for these two values of α shows that the meridional and azimuthal velocity fields are indeed almost identical; the boundary layer in the vorticity is now much more pronounced, showing clearly that the interior is effectively inviscid. The difference between cases (ii) and (iii) for $\alpha = 9.5$ must be attributed to the effects of the $\mathbf{U} \cdot \nabla \mathbf{U}$ term. For case (ii), as we have seen, it is already dominating the dynamics at this value of α . Here, however, it is much less important since E_M is only $\frac{1}{16}$ as large. The contours show much less change with increasing α in this case; the only effect seems to be an increasing localization of the source of poloidal motions, and no region of reversed flow appears.

An interesting aspect of this case was the occurrence of persistent oscillations at all values of α . These motions have frequencies of the order of $4E_M^{\frac{1}{2}}$ and have typical amplitudes (as far as the variations in b^2 are concerned) of about 0.002. Since this is within the error margin of the finite-difference scheme, it is possible that these oscillations are due to some deficiency in the numerical method. However, there is some justification for thinking that they may represent a real lack of stability of the magnetostrophic state. The motions neither grew nor decayed appreciably during the entire course of each run.

In a recent paper, Roberts & Stewartson (1975) have argued that under some circumstances the state of magnetostrophic balance may be unstable to oscillatory disturbances. This may well be the cause of the motions observed here. Their analysis, however, held only for the case in which the oscillation time scale was of the order of the Ohmic decay time. In the present situation, it is hard to see how the fast oscillations can continue to extract energy from the motion since the time scales are so disparate. It would seem likely that the situation resembles that in the Boussinesq approximation, which can be thought of as an average over times long compared with the

acoustic travel time. Such a state is continually 'unstable' to acoustic disturbances, which act to transmit information on the pressure from one region to another. The Taylor oscillations could presumably play such a role here. The question remains open until the advent of analytical models that have validity in parameter ranges relevant to the earth.

A final note should be added regarding the relation between the results presented here and the magnetic fields observed in the earth. There are many features missing from the model: a tilted dipole field and any westward drift are suppressed along with any azimuthal variations. Direct comparison of magnitudes is difficult since realistic values of E and E_M could not be used in the program. However, the parameter $(\Omega\lambda\mu\rho)^{\frac{1}{2}}$, measuring the field strength, is of the order of 30 G, so that we should expect that the earth's field would be in the weakly nonlinear regime if the scaling were correct. Velocity-field comparisons are difficult since we used free boundaries. A typical magnitude of the azimuthal velocity is $10\lambda/L-100\lambda/L$, where L is the core radius: this gives speeds of the order of 1 cm/s, which is not incompatible with velocities inferred from the westward drift. Finally, if E_M is taken as 10^{-7} , typical time scales resulting from the proposed torsional waves would be of the order of decades, which again seems to coincide quite well with some frequencies in the variation of the length of the day. These concatenations clearly suggest the broad correctness of the balances proposed here and in I.

4. Conclusions

The model investigated here provides a first numerical study of the effect of the large-scale flow induced by a global magnetic field that was first investigated theoretically by Malkus & Proctor (1975). It has been shown that if the dynamical effects of the small scales are suppressed the most potent element in the limitation of field growth is the balance between Lorentz and Coriolis forces, at least in parameter ranges relevant to the earth. This is in strong contrast to the recent prescription of Braginskii (1975, 1976), who has argued that in the limit $E_M, E \rightarrow 0$ the asymptotic state is one of high toroidal shear and an absence of magnetic field perpendicular to the axis of rotation away from the boundaries. Our studies showed no such development, and the results for cases (ii) and (iii) show that the system is tending to a state in which Taylor's condition is satisfied and viscosity is unimportant. One disappointment in the work was its failure to distinguish the linear eigenvalue α_0 from the new eigenvalue α_{inviscid} that results if $E, E_M \rightarrow 0$ and Taylor's condition is required to be satisfied by the infinitesimal field (see I). This seems to be because Taylor's condition appears (fortuitously) to be almost satisfied by the linear eigensolution (values of $\int b(\partial a/\partial z) dV$ for all three cases were of the order of $0.01M$). (Some solutions to this problem have been obtained in a simplified geometry by Proctor 1975.) Further, the results suggest that the difficulties that appeared in the analysis of I are a consequence of the special form of f that was chosen, and do not arise in general.

The completion of this work opens up new and more exciting fields of endeavour. There are now several theories of magnetic field limitation in the earth, notably those of Busse (1975) and Roberts & Stewartson (1975), both based on small-scale dynamical consequences, and our own alternative as adumbrated in I. The challenge now is the construction of a theory that includes both large- and small-scale dynamics in a

realistic parameterization that nevertheless avoids detailed treatment of the difficult problem of the small-scale processes in the core. A further area of interest is a solution of the present problem in the limit $E, E_M^{\frac{1}{2}} \rightarrow 0$, when Taylor's condition must be incorporated from the outset. A study of this problem is at present in progress.

This research was performed while the author was a research student at Trinity College, Cambridge, England, and a preliminary report appears in his Ph.D. thesis (Proctor 1975). Grateful thanks are due to Dr H. K. Moffatt for his help and encouragement while this work was in progress, to Prof. W. V. R. Malkus for suggesting the study, and to Dr N. O. Weiss and Dr D. R. Moore for advice on numerical problems. The computations were carried out on the IBM 370/165 of the University Computing Service, Cambridge, England. Thanks are due to the Director for a generous allocation of resources.

Appendix A. Finite-difference representations

All the diffusive terms in the equations were represented by a scheme analogous to the DuFort–Frankel scheme

$$d^2 b_i^n / dx^2 = [b_{i+1}^n + b_{i-1}^n - b_i^{n+1} - b_i^{n-1}] / (\Delta x)^2, \quad (\text{A } 1)$$

which is known to be unconditionally stable. The present scheme is derived from the ideas of MPW, using the fact that

$$D^2 a = -\nabla \times \nabla \times (a \hat{\mathbf{e}}_\phi) \cdot \hat{\mathbf{e}}_\phi. \quad (\text{A } 2)$$

Applying the curl operator twice by integrating round a circuit centred on the point (i, j) we obtain

$$D^2 a_{ij}^n = -R_{ij} [a_{ij}^{n+1} + a_{ij}^{n-1}] + \frac{1}{\Delta r^2} \left[\left(\frac{1+\Delta r}{r_i} \right) a_{j+1,j}^n + \left(\frac{1-\Delta r}{r_i} \right) a_{i-1,j}^n \right] \\ + \frac{1}{r_i^2 \Delta \theta^2} \left[\frac{\sin \theta_{j+1}}{\sin \theta_{j+\frac{1}{2}}} a_{i,j+1}^n + \frac{\sin \theta_{j-1}}{\sin \theta_{j-\frac{1}{2}}} a_{i,j-1}^n \right], \quad (\text{A } 3)$$

where

$$R_{ij} = \frac{1}{\Delta r^2} + \frac{\sin \theta_j}{r_i^2 \Delta \theta^2} \left[\frac{1}{\sin \theta_{j-\frac{1}{2}}} + \frac{1}{\sin \theta_{j+\frac{1}{2}}} \right]$$

and

$$a_{ij}^n = a(i\Delta r, j\Delta \theta; n\Delta t), \quad \text{etc.}$$

This scheme gave linear decay rates correct to four decimal places when used with $N = 10$.

The two nonlinear terms had to be expressed in naive non-conservative forms so as to avoid the inaccuracies mentioned in § 2. The schemes finally decided on were

$$N(a, b)_{ij}^n = [\nabla \times (a \hat{\mathbf{e}}_\phi) \times \nabla \times (b \hat{\mathbf{e}}_\phi) \cdot \hat{\mathbf{e}}_\phi]_{ij}^n \\ = (4r_i^2 \Delta r \Delta \theta)^{-1} \{ (b_{i,j+1}^n - b_{i,j-1}^n + 2\Delta \theta \cot \theta_j b_{ij}^n) [r_i (a_{j+1,j}^n - a_{i-1,j}^n) + 2\Delta r a_{ij}^n] \\ - (a_{i,j+1}^n - a_{i,j-1}^n + 2\Delta \theta \cot \theta_j a_{ij}^n) [r_i (b_{i+1,j}^n - b_{i-1,j}^n) + 2\Delta r b_{ij}^n] \}, \quad (\text{A } 4)$$

$$M(\omega, b)_{ij}^n = [\nabla \times (\omega \hat{\mathbf{e}}_\phi \times \nabla \times (b \hat{\mathbf{e}}_\phi) \cdot \hat{\mathbf{e}}_\phi]_{ij}^n \\ = (4r_i \Delta r \Delta \theta)^{-1} [(\omega_{i+1,j}^n - \omega_{i-1,j}^n) (b_{i,j+1}^n - b_{i,j-1}^n - 2\Delta \theta \cot \theta_j b_{ij}^n) \\ + 2\Delta \theta \cot \theta_j \omega_{ij}^n (b_{i+1,j}^n - b_{i-1,j}^n) - (2\Delta r / r_i) \omega_{ij}^n (b_{i,j+1}^n - b_{i,j-1}^n) \\ - (\omega_{i,j+1}^n - \omega_{i,j-1}^n) (b_{i+1,j}^n - b_{i-1,j}^n + (2\Delta r / r_i) b_{ij}^n)]. \quad (\text{A } 5)$$

Appendix B. Treatment of the Lorentz forces

In implementation of the finite-difference formulation, a difficulty arises in evaluation of the term

$$M(D^2a, a) \quad (\text{B } 1)$$

in (2.2*b*). Although this is in standard form, direct evaluation for $r = 1 - \Delta r$ is not possible since the scheme does not define D^2a at the boundary. Neither is extrapolation possible, since D^2a is discontinuous at $r = 1$. For this reason, (B 1) was replaced by

$$-M(\alpha fb, a) - M(N(\psi, a), a) + M(\partial a / \partial t, a) \quad (\text{B } 2)$$

by substitution in (2.2*a*). This expression can be calculated everywhere since $N(\psi, a)$ contains only first derivatives and can therefore be evaluated correctly by using backward difference formulae at the boundary. The only adverse consequence of using (B 2) is that the variable a must be held at three time levels instead of two; this is not a serious drawback in practice.

REFERENCES

- BRAGINSKIĬ, S. I. 1970 Oscillation spectrum of the hydromagnetic dynamo of the earth. *Geomag. Aero.* **10**, 172–181.
- BRAGINSKIĬ, S. I. 1975 An almost axially symmetrical model of the hydromagnetic dynamo of the earth. I. *Geomag. Aero.* **15**, 149–156.
- BRAGINSKIĬ, S. I. 1976 A nearly symmetrical geodynamo model. *Phys. Earth Planet. Int.* **11**, 191–199.
- BUSSE, F. H. 1975 *Invited Lectures, Geophys. Fluid Dyn. Summer School, Woods Hole, Mass.*
- GREENSPAN, H. P. 1974 On α -dynamoes. *Stud. Appl. Math.* **43**, 35–43.
- JEPPS, S. A. 1975 Numerical models of hydromagnetic dynamoes. *J. Fluid Mech.* **67**, 625–646.
- MALKUS, W. V. R. & PROCTOR, M. R. E. 1975 The macrodynamics of α -effect dynamoes in rotating fluid systems. *J. Fluid Mech.* **67**, 417–444.
- MOORE, D. R., PECKOVER, R. S. & WEISS, N. O. 1973 Difference methods for time dependent two dimensional convection. *Comp. Phys. Comm.* **6**, 198–220.
- PROCTOR, M. R. E. 1975 Non-linear mean field dynamo models and related topics. Ph.D. thesis, University of Cambridge.
- ROBERTS, P. H. 1972 Kinematic dynamo models. *Phil. Trans. Roy. Soc. A* **272**, 663–698.
- ROBERTS, P. H. & SOWARD, A. M. 1972 Magnetohydrodynamics of the earth's core. *Ann. Rev. Fluid Mech.* **4**, 117–154.
- ROBERTS, P. H. & STEWARTSON, K. 1975 On double-roll convection in a rotating magnetic system. *J. Fluid Mech.* **68**, 447–466.
- TAYLOR, J. B. 1963 The magnetohydrodynamics of a rotating fluid and the earth's dynamo problem. *Proc. Roy. Soc. A* **274**, 274–283.
- WEIR, A. D. 1976 Axisymmetric convection in a rotating sphere. Part 1. Stress-free surface. *J. Fluid Mech.* **75**, 49–79.